Heterometallic Adducts of $[Rh_6(CO)_{15}C]^{2-}$, including the Novel Double- and Triple-Decker Sandwich Compounds $[Ag_n\{Rh_6(CO)_{15}C\}_2]^{(4-n)-}$ (n = 1 and 3) and $[Ag_n\{Rh_6(CO)_{15}C\}_3]^{(6-n)-}$ (n = 2 and 4) and the *X*-Ray Structural Characterisation of $[PPh_4]_3[Ag\{Rh_6(CO)_{15}C\}_2]$ †

Brian T. Heaton * and Luisella Strona
Chemical Laboratory, University of Kent at Canterbury, Canterbury CT2 7NH
Secondo Martinengo * and Donatella Strumolo
Centro di Studio Sulla Sintesi e la Struttura dei Composti dei Metalli di Transizione nei Bassi Strati di Ossidazione del CNR and Istituto di Chimica Generale ed Inorganica, via G. Venezian 21, 20133 Milano, Italy
Vincenzo G. Albano * and Dario Braga
Istituto Chimico 'G. Ciamician' dell'Università, via F. Selmi 2, 40126 Bologna, Italy

Multinuclear n.m.r. measurements have been used to establish the formation of the following new adducts of $[Rh_6(CO)_{15}C]^{2-}$ by capping the trigonal face of the Rh_6 trigonal prism: $[\{M(PEt_3)\}\{Rh_6(CO)_{15}C\}]^-$ (M = Ag or Au), $[Ag_n\{Rh_6(CO)_{15}C\}_2]^{(4-n)-}$ (n = 1 or 3), $[Ag_n\{Rh_6(CO)_{15}C\}_3]^{(6-n)-}$ (n = 2 or 4), $[Ag_n\{Rh_6(CO)_{15}C\}_n]^{n-}$ (n > 3), and $[Ag_2\{Rh_6(CO)_{15}C\}]$. There is no evidence for dissociation of any of these species on the n.m.r. time-scale, whereas n.m.r. spectra suggest that dissociation of $[Cu(NCMe)]^+$ occurs in $[\{Cu(NCMe)\}_n\{Rh_6(CO)_{15}C\}]^{(2-n)-}$ (n = 1 or possibly 2) both at room and low temperature. *X*-Ray crystallographic analysis of $[Ag\{Rh_6(CO)_{15}C\}_2]^{3-}$ shows that a silver atom is sandwiched between trigonal faces of two staggered Rh_6 trigonal-prismatic units and the nature of the silver–rhodium interaction is discussed.

The progressive capping of either triangular or square faces of metal polyhedra in high nuclearity carbonyl clusters can be carried out in a controlled way to give good yields of higher nuclearity carbonyl clusters.[1] This process, which resembles surface reconstruction on metals, can use either nucleophilic or electrophilic capping reagents but the factors controlling the charge on the face to be capped are presently not well understood.

Previous work suggested that the trigonal face in the Rh_6 trigonal prismatic cluster, $[Rh_6(CO)_{15}C]^{2-}$, was susceptible to electrophilic attack since protonation occurred at this site [2] and the step-wise addition of $[Cu(NCMe)_4]BF_4$ gave evidence for the formation of both mono- and bis-copper derivatives with the latter cluster, $[\{Cu(NCMe)\}_2\{Rh_6(CO)_{15}C\}]$, having been shown by *X*-ray crystallography to have two $[Cu(NCMe)]^+$ fragments capping both trigonal faces.[3] In order to extend these observations, we carried out reactions of $[Rh_6(CO)_{15}C]^{2-}$ with other electrophilic species and now report multinuclear (^{13}C, ^{31}P, ^{103}Rh, $^{13}C\{^{31}P\}$, and $^{13}C\{^{103}Rh\}$) n.m.r. evidence for the formation of $[\{M(PEt_3)\}\{Rh_6(CO)_{15}C\}]^-$ (M = Ag or Au); there is no evidence for co-ordination of a second $[M(PEt_3)]^+$ group. However, by using lightly stabilised Ag^I, *i.e.* $Ag[BF_4]$ in acetone solution, thereby exposing both co-ordination sites on Ag^I, we find evidence for the formation of a remarkable series of oligomers, which contain Rh_6 trigonal prismatic units bridged by Ag^I; $[Ag\{Rh_6(CO)_{15}C\}_2]^{3-}$ has been characterised by *X*-ray crystallography and shown to contain silver bridging two staggered trigonal prismatic $[Rh_6(CO)_{15}C]^{2-}$ units *via* trigonal faces.

† Tris(tetraphenylphosphonium) 1,2,3,1′,2′,3′-μ_6-argentio-bis[μ_6-carbido-nona-μ-carbonyl-hexacarbonylhexarhodate(3−) (9*Rh*–*Rh*)].

Supplementary data available (No. SUP 23664, 60 pp.): thermal parameters, observed and calculated structure factors. See Notices to Authors No. 7, *J. Chem. Soc., Dalton Trans.*, 1981, Index issue.

Results and Discussion

Adducts of $[Rh_6(CO)_{15}C]^{2-}$ *with* $[ML]^+$ (M = Cu, L = NCMe; M = Ag *or* Au, L = PEt_3).—Addition of $[Au(PEt_3)Cl]$ to an acetone solution of $[NMe_3(CH_2Ph)]_2[Rh_6(CO)_{15}C]$ results in the formation of $[\{Au(PEt_3)\}\{Rh_6(CO)_{15}C\}]^-$ (1). The formation of (1) is only complete when the ratio of Au : Rh is *ca.* 2 : 1, but there is no evidence for the formation of $[\{Au(PEt_3)\}_2\{Rh_6(CO)_{15}C\}]$ even on addition of a *ca.* ten-fold excess of $[Au(PEt_3)Cl]$.

Consistent with the $[Au(PEt_3)]^+$ group capping a trigonal Rh_3 face (Figure 1), the ^{31}P n.m.r. spectrum of (1) at 25 °C is a quartet [$\delta(^{31}P)$ +55.5 p.p.m.; $^2J(^{31}P-^{103}Rh_Y)$ = 5.8 Hz] and the ^{103}Rh n.m.r. spectrum at −80 °C consists of a doublet due to Rh_Y [$\delta(^{103}Rh_Y)$ −433 p.p.m.; $^2J(^{31}P-^{103}Rh_Y)$ = 5.8 Hz] and a singlet due to Rh_X [$\delta(^{103}Rh_X)$ −272 p.p.m.]. The ^{13}C and $^{13}C\{^{103}Rh\}$ n.m.r. spectra (Figure 2) are also entirely in accord with the structure shown in Figure 1. Thus, there are three equally intense resonances due to the three bridging carbonyls (C^cO, C^dO, and C^eO in Figure 1) and two resonances due to the two inequivalent terminal carbonyls (C^aO and C^bO) which may be unambiguously assigned by specific ^{103}Rh decoupling [Figure 2(*a*) and (*b*)]. The resonance due to C^aO consists of a doublet of doublets at 193.7 p.p.m. and specific ^{103}Rh decoupling shows that the small doublet splitting (4.9 Hz) must be due to $^2J(^{103}Rh_Y-^{13}C^aO)$. This value is similar to that previously attributed to $^2J(^{103}Rh-^{13}CO)$ in $[Rh_6(CO)_{15}C]^{2-}$ [4] and, although such two-bond couplings are usually not observed in rhodium carbonyl clusters, probably arises because of the rather large $RhRhCO_t$ (t = terminal) angle (140.5°).[5] The absence of the corresponding coupling constant to the other set of terminal carbonyls in (1), $^2J(^{103}Rh_X-^{13}C^bO)$, is probably due to the occupancy of the $(Rh_Y)_3$ face by the $[Au(PEt_3)]^+$ group which causes the terminal carbonyls, C^bO, to become more coplanar with the $(Rh_Y)_3$ plane thus decreasing the $Rh_XRh_YC^b$ angle. The resonance due to C^dO at 230.6 p.p.m. appears as a triplet of doublets. The triplet arises from accidental equivalence of

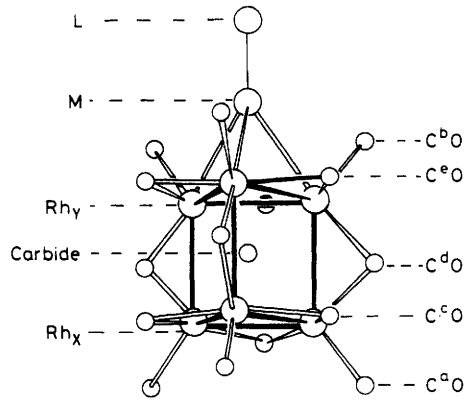

Figure 1. Schematic structure of the adducts $[\{ML\}\{Rh_6(CO)_{15}C\}]^-$ (M = Cu, L = NCMe; M = Ag or Au, L = PEt_3)

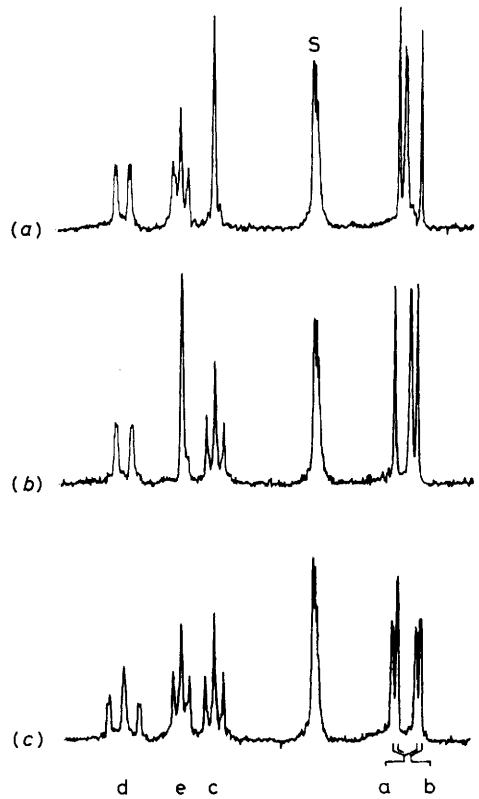

Figure 2. The (*a*) ^{13}C-$\{^{103}Rh_X\}$, (*b*) ^{13}C-$\{^{103}Rh_Y\}$, and (*c*) ^{13}C n.m.r. spectra of $[\{Au(PEt_3)\}\{Rh_6(CO)_{15}C\}]^-$ (*ca.* 40% ^{13}CO) in $[^2H_6]$-acetone at −80 °C (see Figure 1 for assignments), S = solvent

$^1J(^{103}Rh_X-C^dO)$ and $^1J(^{103}Rh_Y-C^dO)$ = 46.9 Hz; the doublet splitting, which clearly remains in the ^{13}C-$\{^{103}Rh\}$ spectra, has been shown to be due to $^3J(^{31}P-C^dO)$ = 6.8 Hz by ^{13}C-$\{^{31}P\}$ measurements. An approximate *trans* configuration of these groups probably also accounts for this being the only phosphorus–carbon coupling constant observed in (1).

The carbide resonance in (1) occurs at slightly higher frequency than in $[Rh_6(CO)_{15}C]^{2-}$ and, although complicated in the undecoupled ^{13}C n.m.r. spectrum, becomes a simple quartet on decoupling either Rh_X or Rh_Y. It should be noted that, although the values of $^1J(Rh_X-C_{carbide})$ = 10.7 and $^1J(Rh_Y-C_{carbide})$ = 12.7 Hz are only slightly different, the larger coupling is found for the capped $(Rh_Y)_3$ face which is similar to that found in $[Rh_6H(CO)_{15}C]^-$.[2] These n.m.r. data are summarised in Table 1.

Table 1. Comparison of n.m.r. data for $[Rh_6(CO)_{15}C]^{2-}$ (5) and adducts of the type $[\{ML\}\{Rh_6(CO)_{15}C\}]^-$ in acetone solution

		ML		
	(5)	H	Au(PEt_3)	Ag(PEt_3)
T/°C	−79	−25	−80	−80
δ(C^aO)/p.p.m.	196.9	193.3	193.7	
δ(C^bO)/p.p.m.	196.9	189.6	193.1	
δ(C^cO)/p.p.m.	224.0	216.0	218.7	
δ(C^dO)/p.p.m.	235.4	225.1	230.6	
δ(C^eO)/p.p.m.	224.0	223.5	223.6	
$\delta(C_{carbide})$/p.p.m.	264.0	291.2	285.3	
$^1J(Rh_X-C^aO)$/Hz	79.3	71.3	77.2	
$^1J(Rh_Y-C^bO)$/Hz	79.3	78.1	74.2	
$^1J(Rh_X-C^cO)$/Hz	30.5	30.3	30.8	
$^1J(Rh_X-C^dO)$/Hz	51.9	58.0	46.9	
$^1J(Rh_Y-C^dO)$/Hz	51.9	32.0	46.9	
$^1J(Rh_Y-C^eO)$/Hz	30.5	25.4	27.3	
$^1J(Rh_X-C_{carbide})$/Hz	14.0	10.0	10.7	
$^1J(Rh_Y-C_{carbide})$/Hz	14.0	15.0	12.7	
$^2J(Rh_Y-C^aO)$/Hz	3.9	3.9	4.9	
$^2J(Rh_X-C^bO)$/Hz	3.9	3.9	0	
$^2J(P-Rh_Y)$/Hz	—	—	5.8	3.9
$^3J(P-C^dO)$/Hz	—	—	6.8	
δ(Rh_X)/p.p.m.	−313	−144	−272	−283
δ(Rh_Y)/p.p.m.	−313	−412	−433	−473
δ(P)/p.p.m.			+55.5 *	+36.6
$^1J(^{107}Ag-P)$/Hz				497
$^1J(^{109}Ag-P)$/Hz				574

* At 25 °C.

The formation of $[\{Ag(PEt_3)\}\{Rh_6(CO)_{15}C\}]^-$ (2) results from the related reaction of $[\{Ag(PEt_3)Br\}_4]$ with $[NMe_3(CH_2Ph)]_2[Rh_6(CO)_{15}C]$ in acetone solution at room temperature. Formation of (2) is only complete at a ratio $[\{Ag(PEt_3)Br\}_4]$:$[Rh_6(CO)_{15}C]^{2-}$ of *ca.* 1 : 2 but this solution is stable only at low temperature (−10 °C) and, on standing at room temperature, a presently uncharacterised red species is formed at a ratio $[\{Ag(PEt_3)Br\}_4]$:$[Rh_6(CO)_{15}C]^{2-}$ of 1 : 1. Nevertheless, n.m.r. measurements clearly establish the formation of (2). Thus, ^{103}Rh n.m.r. spectra at −80 °C show two equally intense peaks at −283 and −473 p.p.m. due to Rh_X and Rh_Y respectively. The low-frequency resonance is clearly broader than the other resonance and this must be due to unresolved coupling to silver and phosphorus. The ^{31}P n.m.r. spectrum at −78 °C consists of two doublets, due to silver coupling [δ(^{31}P) +36.6 p.p.m.; $^1J(^{107}Ag-^{31}P)$ = 497, $^1J(^{109}Ag-^{31}P)$ = 574 Hz], which are further split into quartets $[^2J(^{103}Rh_Y-^{31}P)$ = 3.9 Hz].

Adduct formation with Cu^I is much less favourable than with Ag^I and Au^I compounds and there is *no* evidence for the formation of $[\{Cu(PEt_3)\}_{2-x}\{Rh_6(CO)_{15}C\}]^{x-}$ (x = 0 or 1) on reaction of $[\{Cu(PEt_3)Cl\}_4]$ with $[NMe_3(CH_2Ph)]_2[Rh_6(CO)_{15}C]$ in acetone solution.

Compared with the unambiguous n.m.r. evidence for adduct formation of $[Rh_6(CO)_{15}C]^{2-}$ with $[M(PEt_3)]^+$ (M = Ag or Au) and with H^+,[2] the n.m.r. evidence for the formation of $[\{Cu(NCMe)\}\{Rh_6(CO)_{15}C\}]^-$ (3) is less convincing. Addition of $[Cu(NCMe)_4]^+$ (1 mol) to an acetone solution of $[NMe_3(CH_2Ph)]_2[Rh_6(CO)_{15}C]$ (1 mol) results in a shift of the ^{13}CO and carbide resonances to lower and higher frequencies respectively, but there is *no* evidence for inequivalence of the two triangular planes. The ^{13}C spectrum of (3) at −83 °C in the carbonyl region consists of one doublet

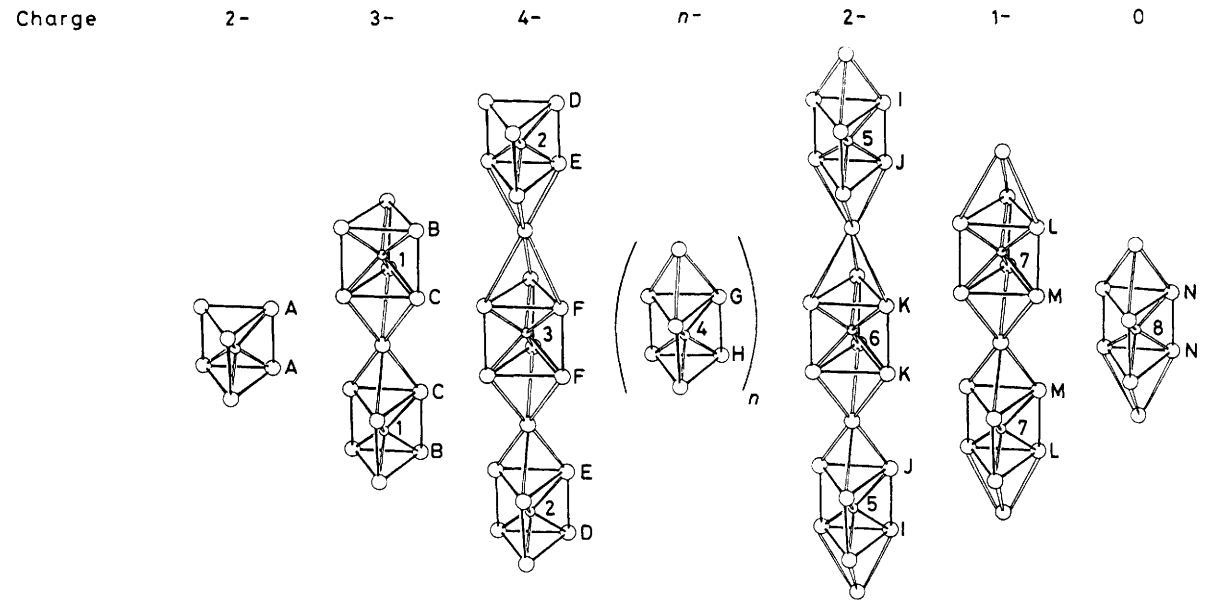

Compound	(5)	(6)	(7)	(8)	(9)	(10)	(11)
$[Rh_6(CO)_{15}C]^{2-}$	1	2	3	1	3	2	1
Ag^+	0	1	2	1	4	3	2*

(*Partial formation: reaction is complete at a ratio of 1:3)

Figure 3. $[Rh_6(CO)_{15}C]^{2-}/Ag^+$ adducts formed on progressive addition of $Ag[BF_4]$

(194.3 p.p.m.) and two triplets (221.4 and 230.5 p.p.m. of relative intensity 2 : 1), due to the terminal and edge-bridging carbonyls respectively, and the carbide resonance occurs at 281.8 p.p.m. as a symmetrical septet $^1J(Rh-C_{carbide}) = 13.2$ Hz; all these resonances collapse to single lines on low-power irradiation at *one* rhodium frequency [$\delta(^{103}Rh) -307$ p.p.m.]. It seems unlikely that there are accidental coincidences in both the ^{13}C and ^{103}Rh resonances and in order to explain the n.m.r. spectra being simpler than expected, we prefer to involve inter-exchange of the $[Cu(NCMe)]^+$ group, equation (i). This is supported by the large shifts found for

$$[Rh_6(CO)_{15}C]^{2-} + [Cu(NCMe)_4]^+ \rightleftharpoons [\{Cu(NCMe)\}\{Rh_6(CO)_{15}C\}]^- + 3MeCN \quad (i)$$

the carbide resonance on changing the temperature and/or the solvent. At room temperature in acetonitrile, $\delta(C_{carbide}) =$ 268.9 p.p.m. due to partial displacement of the above equilibrium to the right, whereas at lower temperatures (−30 °C) the $T\Delta S$ term favours the left-hand side of equation (i) and $\delta(C_{carbide}) = 264.8$ p.p.m., which is close to that found for $[Rh_6(CO)_{15}C]^{2-}$ [$\delta(C_{carbide}) = 264.0$ p.p.m.];[4] similarly, in acetone solution at −80 °C, displacement of the above equilibrium to the right occurs and $\delta(C_{carbide}) = 281.8$ p.p.m.

Similar spectra, but with different carbonyl, carbide, and rhodium chemical shifts are also found for $[\{Cu(NCMe)\}_2\{Rh_6(CO)_{15}C\}]$ (4), both at room and low temperature (see Experimental section). This is consistent with the solid-state structure of (4)[3] but fragmentation of $[Cu(NCMe)]^+$ could also be occurring. It is worth noting that, compared to $[NMe_3(CH_2Ph)]_2[Rh_6(CO)_{15}C]$, the i.r. bands of (3) and (4) in acetone solution move progressively to higher frequencies due to the reduction in negative charge per carbonyl.*

Adducts of $[Rh_6(CO)_{15}C]^{2-}$ *with* Ag^+.—The nature of the products formed on addition of $Ag[BF_4]$ to an acetone solution of $[NMe_3(CH_2Ph)]_2[Rh_6(CO)_{15}C]$ depends critically upon the ratio $Ag^+ : [Rh_6(CO)_{15}C]^{2-}$. By monitoring continuously the ^{13}C and $^{13}C-\{^{103}Rh\}$ n.m.r. spectra of both $[Rh_6(^{13}CO)_{15}C]^{2-}$ and $[Rh_6(CO)_{15}{}^{13}C]^{2-}$, as well as the ^{103}Rh n.m.r. spectra of $[Rh_6(CO)_{15}C]^{2-}$, after careful incremental additions of $Ag[BF_4]$, it has been possible to obtain an overall understanding of the resulting species, which are summarised in Figure 3, together with the $Ag^+ : [Rh_6(CO)_{15}C]^{2-}$ ratios; in the case of the first formed product, $[Ag\{Rh_6(CO)_{15}C\}_2]^{3-}$ (6), it was possible to obtain crystals, which have been structurally characterised by *X*-ray crystallography.

X-Ray Structure of the Trianion $[Ag\{Rh_6(CO)_{15}C\}_2]^{3-}$ (6).—The crystal consists of tetraphenylphosphonium cations and $[Ag\{Rh_6(CO)_{15}C\}_2]^{3-}$ anions. The unit cell contains two $[Ag\{Rh_6C(CO)_{15}\}_2]^{3-}$ anions with the silver atoms at inversion centres, therefore only one half of each anion is crystallographically independent. The three independent tetraphenylphosphonium cations occupy general positions.

The geometry of the anion of (6) is shown in Figure 4. It consists of two Rh_6 prismatic units which sandwich a silver atom between two triangular faces. An inversion centre relates the two Rh_6 prisms, which are staggered with respect to each other and the resulting idealised symmetry of the whole anion is D_{3h}. Interstitial carbon atoms are in the prismatic cavities and 30 carbonyl ligands are co-ordinated on the prism surfaces. On each prismatic unit there are nine carbonyls bridging all edges of the prism and each rhodium has one terminal carbonyl group; this is the same arrangement of

* Carbonyl bands [ν(CO)/cm^{-1}]: $[NMe_3(CH_2Ph)]_2[Rh_6(CO)_{15}C]$ 1 995, 1 990 (sh), and 1 843; $[NMe_3(CH_2Ph)][\{Cu(NCMe)\}\{Rh_6(CO)_{15}C\}]$ 2 010 and 1 863; $[\{Cu(NCMe)\}_2\{Rh_6(CO)_{15}C\}]$ 2 027 and 1 881.

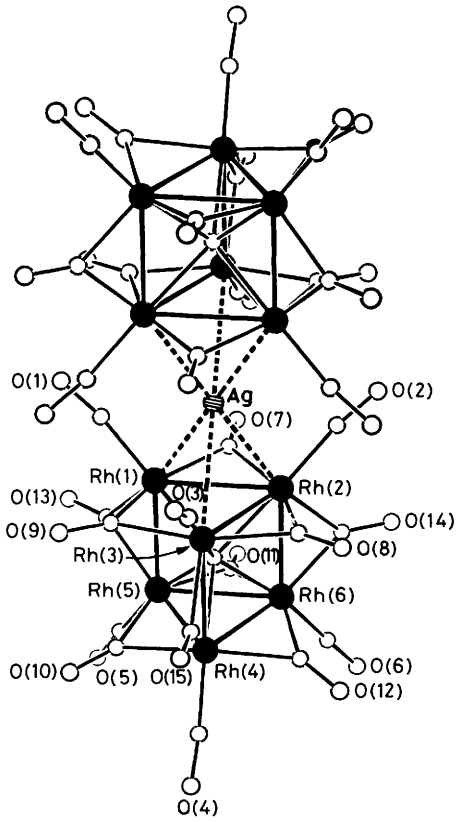

Figure 4. The anion $[Ag\{Rh_6(CO)_{15}C\}_2]^{3-}$ showing the atom labelling. The carbon atoms of the CO ligands, not labelled, bear the same numbers as the corresponding oxygens

carbonyls as that found in the parent dianion, $[Rh_6(CO)_{15}C]^{2-}$, the only variation being slight angular deformations of the inner ligands (see Table 2).

The two semi-independent anions are substantially equivalent and the slight differences in bond distances do not seem to be chemically significant, therefore only the mean values taken from the two anions will be discussed.

The Rh_6 prisms conform to the idealised D_{3d} symmetry of the parent dianion within experimental error. The average Rh–Rh distances in the outer and inner triangles are equal [2.780(1) and 2.781(1) Å respectively] showing no effects attributable to the sandwiched silver atom. These distances are barely different from the values in the parent dianion $[Rh_6C(CO)_{15}]^{2-}$ [2.776(3) Å] [5] and the copper derivative $[\{Cu(NCMe)\}_2\{Rh_6(CO)_{15}C\}]$ [2.765(1) Å].[3] Similarly, the inter-basal Rh_B–Rh_C distances [2.826(1) Å] are strictly comparable with the corresponding values in the aforementioned related species [2.817(2) and 2.810(1) Å, respectively].[3,4] The values in the present trianion (6) are closer to those in the parent dianion (5), with the small but significant shortenings found for $[\{Cu(NCMe)\}_2\{Rh_6(CO)_{15}C\}]$ being attributable to the disappearance of the anionic charge. As expected, the Rh–C(carbide) interaction [2.136(4) Å] is almost equal to the value in $[Rh_6(CO)_{15}C]^{2-}$ [2.134(4) Å] [4] and only slightly longer than in $[\{Cu(NCMe)\}_2\{Rh_6(CO)_{15}C\}]$ [2.123(3) Å].[3]

A major feature of this new molecular architecture is the silver–rhodium interaction. The Ag–Rh distances are in the range 2.870(1)—3.052(1) Å; the silver atoms are not equidistant from the rhodium atoms and the degree of asymmetry is different in the two independent anions. On the contrary, the average values in the two anions are strictly comparable (2.979 and 2.986 Å) suggesting that packing forces are responsible for the variations in bond lengths. The overall mean value of Ag–Rh (2.98 Å) should be compared with the copper–rhodium distance in $[\{Cu(NCMe)\}_2\{Rh_6(CO)_{15}C\}]$ (2.66 Å) and the radii of the three elements in the bulk metals (Rh 1.34, Cu 1.28, and Ag 1.44 Å).[6] These figures show that while the copper–rhodium bond length is strictly comparable with the sum of the metallic radii, the silver–rhodium distance is 0.20 Å longer.

The silver–rhodium interaction can be viewed as the electrostatic interaction between a cation sandwiched between two dianions. The observed Ag–Rh distances are then a compromise between attractive and repulsive cation–anion and anion–anion interactions with the lack of directionality in these interactions accounting for the observed deformations in the observed Ag–Rh distances. However, as suggested by the adduct formation with H^+,[2] it is also possible that the Rh_6 trigonal prismatic unit can function as a sophisticated ligand by donating a pair of electrons from either one or both trigonal faces, thus allowing linear co-ordination with d^{10} metals. This view of the bonding in the adducts of $[Rh_6(CO)_{15}C]^{2-}$ is in keeping with the recent proposal from i.r. studies that the carbide atom bonds *via sp* hybrid orbitals to a set of metal orbitals on the Rh_3 trigonal face [7] which are similar to those used on the opposite side of the face for adduct formation.

Additionally, there seems to be further stabilisation from the six terminal carbonyls on the inner layers encapsulating and weakly interacting with the silver ion (average Ag · · · CO contact 3.17 Å). The bond distances of the terminal carbonyls on the inner and outer faces are not sufficiently well determined to discuss the slight differences between them [overall average values, Rh–C 1.858(4) and C–O 1.167(8) Å] but the RhCO bond angles [170.7(5) and 177.1(5)° for the inner and outer faces respectively] are significantly different; these values should be compared with those found in $[Rh_6(CO)_{15}C]^{2-}$ [177.7(5)°] and in $[\{Cu(NCMe)\}_2\{Rh_6(CO)_{15}C\}]$ [174.3(5)°], which have empty and capped Rh_3 faces respectively. Thus, the capping atom is responsible for the RhCO bending, which originates from a slight but significant capping metal–carbonyl interaction, with the interaction being greater for silver than copper.

The bridging groups show the following mean Rh–C and C–O values for the basal and inter-basal groups: 2.09, 1.18 and 2.03, 1.18 Å, respectively (see Table 2). These values compare well with those found for (5) and $[\{Cu(NCMe)\}_2\{Rh_6(CO)_{15}C\}]$.

Spectroscopic Studies of the Adducts of $[Rh_6(CO)_{15}C]^{2-}$ *with* Ag^+ *in Solution.*—For all the species shown in Figure 3 the i.r. spectra in acetone solution have a similar appearance and ν(CO) shifts progressively from 1 995, 1 990 (sh), and 1 843 to 2 030 and 1 882 cm^{-1} on going from $[Rh_6(CO)_{15}C]^{2-}$ (5) to $[Ag_2\{Rh_6(CO)_{15}C\}]$ (11), with $[Ag\{Rh_6(CO)_{15}C\}_2]^{3-}$ (6) having bands at 2 005vs, 1 861s, 1 830m, and 1 815m cm^{-1}. However, it should be noted that, with increasing additions of Ag^+ {up to a ratio Ag^+: $[Rh_6(CO)_{15}C]^{2-}$ of ≤1 : 1}, there is an enormous increase in viscosity of the solution due to the increasing molecular weights of the oligomers which are formed by the Ag^+ *first bridging* Rh_6 trigonal prismatic units *via* trigonal faces. On further addition of $Ag[BF_4]$, the viscosity of the solution gradually returns to normal; this results from fragmentation of the oligomers due to Ag^+ capping outer Rh_3 faces of the Rh_6 trigonal prism until eventually $[Ag_2\{Rh_6(CO)_{15}C\}]$ (11) is formed.

The first heterometallic species formed on addition of $Ag[BF_4]$ to $[Rh_6(CO)_{15}C]$ is (6) (see Figure 3) and is the only species present at a ratio Ag^+ : $[Rh_6(CO)_{15}C]^{2-}$ of 1 : 2.

Table 2. Distances (Å) and relevant angles (°) with estimated standard deviations in parentheses

Ag(1)–Rh(1)	3.005(1)	Ag(2)–Rh(7)	2.870(1)	Rh(4)–C(O1)	2.14(1)	Rh(10)–C(O2)	2.14(2)
Ag(1)–Rh(2)	2.945(1)	Ag(2)–Rh(8)	3.035(1)	Rh(5)–C(O1)	2.14(1)	Rh(11)–C(O2)	2.14(1)
Ag(1)–Rh(3)	2.988(1)	Ag(2)–Rh(9)	3.052(1)	Rh(6)–C(O1)	2.13(1)	Rh(12)–C(O2)	2.13(2)
Rh(1)–Rh(2)	2.784(1)	Rh(7)–Rh(8)	2.782(1)	Ag(1) · · · C(1)	3.19(2)	Ag(2) · · · C(16)	3.01(1)
Rh(1)–Rh(3)	2.757(1)	Rh(7)–Rh(9)	2.787(1)	Rh(1)–C(1)	1.86(2)	Rh(7)–C(16)	1.84(1)
Rh(1)–Rh(5)	2.820(1)	Rh(7)–Rh(11)	2.828(1)	Ag(1) · · · C(2)	3.11(2)	Ag(2) · · · C(17)	3.24(2)
Rh(2)–Rh(3)	2.766(1)	Rh(8)–Rh(9)	2.750(1)	Rh(2)–C(2)	1.87(1)	Rh(8)–C(17)	1.87(1)
Rh(2)–Rh(6)	2.832(1)	Rh(9)–Rh(10)	2.819(1)	Ag(1) · · · C(3)	3.19(2)	Ag(2) · · · C(18)	3.28(11)
Rh(3)–Rh(4)	2.827(1)	Rh(10)–Rh(12)	2.784(1)	Rh(3)–C(3)	1.88(1)	Rh(9)–C(18)	1.87(2)
Rh(4)–Rh(5)	2.793(1)	Rh(10)–Rh(11)	2.768(1)	Rh(4)–C(4)	1.86(1)	Rh(10)–C(19)	1.84(1)
Rh(4)–Rh(6)	2.784(1)	Rh(12)–Rh(8)	2.829(1)	Rh(5)–C(5)	1.87(2)	Rh(11)–C(20)	1.84(1)
Rh(5)–Rh(6)	2.762(1)	Rh(12)–Rh(11)	2.791(1)	Rh(6)–C(6)	1.85(2)	Rh(12)–C(21)	1.85(2)
Rh(1)–C(O1)	2.13(1)	Rh(7)–C(O2)	2.15(2)	Rh(1)–C(7)	2.14(1)	Rh(7)–C(22)	2.13(1)
Rh(2)–C(O1)	2.13(1)	Rh(8)–C(O2)	2.13(1)	Rh(2)–C(7)	2.11(1)	Rh(8)–C(22)	2.06(1)
Rh(3)–C(O1)	2.14(1)	Rh(9)–C(O2)	2.14(1)	Rh(2)–C(8)	2.11(1)	Rh(8)–C(23)	2.09(1)
Rh(3)–C(8)	2.07(1)	Rh(9)–C(23)	2.09(1)	C(1)–O(1)	1.18(2)	C(16)–O(16)	1.18(2)
Rh(1)–C(9)	2.09(1)	Rh(7)–C(24)	2.06(1)	C(2)–O(2)	1.16(2)	C(17)–O(17)	1.17(2)
Rh(3)–C(9)	2.09(1)	Rh(9)–C(24)	2.07(1)	C(3)–O(3)	1.14(2)	C(18)–O(18)	1.15(2)
Rh(4)–C(10)	2.09(1)	Rh(10)–C(25)	2.08(1)	C(4)–O(4)	1.17(2)	C(19)–O(19)	1.18(2)
Rh(5)–C(10)	2.11(1)	Rh(11)–C(25)	2.06(1)	C(5)–O(5)	1.16(2)	C(20)–O(20)	1.18(2)
Rh(5)–C(11)	2.10(1)	Rh(11)–C(26)	2.09(1)	C(6)–O(6)	1.17(2)	C(21)–O(21)	1.17(2)
Rh(6)–C(11)	2.06(1)	Rh(12)–C(26)	2.08(1)	C(7)–O(7)	1.15(2)	C(22)–O(22)	1.20(2)
Rh(4)–C(12)	2.11(2)	Rh(10)–C(27)	2.09(1)	C(8)–O(8)	1.18(2)	C(23)–O(23)	1.18(2)
Rh(6)–C(12)	2.08(1)	Rh(12)–C(27)	2.07(1)	C(9)–O(9)	1.18(2)	C(24)–O(24)	1.22(2)
Rh(1)–C(13)	2.08(1)	Rh(7)–C(28)	2.03(1)	C(10)–O(10)	1.16(2)	C(25)–O(25)	1.18(2)
Rh(5)–C(13)	2.01(2)	Rh(11)–C(28)	2.00(1)	C(11)–O(11)	1.18(2)	C(26)–O(26)	1.20(2)
Rh(2)–C(14)	2.04(1)	Rh(8)–C(29)	2.04(1)	C(12)–O(12)	1.16(2)	C(27)–O(27)	1.17(2)
Rh(6)–C(14)	2.00(1)	Rh(12)–C(29)	2.01(1)	C(13)–O(13)	1.16(2)	C(28)–O(28)	1.22(2)
Rh(3)–C(15)	2.07(1)	Rh(9)–C(30)	2.04(1)	C(14)–O(14)	1.17(2)	C(29)–O(29)	1.18(2)
Rh(4)–C(15)	2.01(1)	Rh(10)–C(30)	2.03(1)	C(15)–O(15)	1.16(2)	C(30)–O(30)	1.18(2)
Rh(1)–C(1)–O(1)	171(1)	Rh(7)–C(16)–O(16)	172(1)	Rh(5)–C(5)–O(5)	178(1)		
Rh(2)–C(2)–O(2)	170(1)	Rh(8)–C(17)–O(17)	170(1)	Rh(6)–C(6)–O(6)	179(1)		
Rh(3)–C(3)–O(3)	171(1)	Rh(9)–C(18)–O(18)	170(1)	Rh(5)–Rh(1)–C(1)	135(1)		
Rh(4)–C(4)–O(4)	175(1)	Rh(10)–C(19)–O(19)	177(1)	Rh(6)–Rh(2)–C(2)	135(1)		
Rh(11)–C(20)–O(20)	177(1)	Rh(4)–Rh(3)–C(3)	135(1)	Rh(10)–Rh(9)–C(18)	135(1)		
Rh(12)–C(21)–O(21)	177(1)	Rh(3)–Rh(4)–C(4)	139(1)	Rh(9)–Rh(10)–C(19)	143(1)		
Rh(11)–Rh(7)–C(16)	133(1)	Rh(1)–Rh(5)–C(5)	143(1)	Rh(7)–Rh(11)–C(20)	140(1)		
Rh(12)–Rh(8)–C(17)	136(1)	Rh(2)–Rh(6)–C(6)	142(1)	Rh(8)–Rh(12)–C(21)	139(1)		

Inspection of Figure 4 shows there to be five sets of equally abundant carbonyls with three sets of edge-bridging (C^7O, C^8O, $C^9O = C^hO$; $C^{13}O$, $C^{14}O$, $C^{15}O = C^iO$; $C^{10}O$, $C^{11}O$, $C^{12}O = C^jO$) and two sets of terminal carbonyls (C^4O, C^5O, $C^6O = C^fO$; C^1O, C^2O, $C^3O = C^gO$). Consistent with this structure, the ^{13}C n.m.r. spectrum, both at −80 and 25 °C, contains three equally intense edge-bridging resonances and two equally intense doublets due to the terminal carbonyls. The direct rhodium n.m.r. spectrum of (6) at −80 °C showed two equally intense rhodium resonances and, as their chemical shifts (−278 and −423 p.p.m.) are very similar to those found for (1) and (2) see above, they can be assigned to Rh_B and Rh_C (see Figure 3) respectively. This then allowed, through ^{13}C-{^{103}Rh} measurements, a complete assignment of the ^{13}C n.m.r. spectrum of (6).*

Further addition of $Ag[BF_4]$ to the acetone solution of (6) caused the rhodium resonances due to Rh_B and Rh_C to decrease in intensity and to be replaced by three new equally intense resonances due to $[Ag_2\{Rh_6(CO)_{15}C\}_3]^{4-}$ (7) at −279, −363, and −433 p.p.m., which have been assigned to Rh_D, Rh_F, and Rh_E respectively (see below). These resonances are too close together to allow specific spin-decoupling measurements of the ^{13}C spectrum, which is very complicated in the carbonyl region because of the complex structure of (7) and because of our inability to obtain (7) on its own in solution. Further addition of $Ag[BF_4]$ gives $[Ag_n\{Rh_6(CO)_{15}C\}_n]^{n-}$ (8), where $n > 3$. In this case, although there are many slightly inequivalent sets of carbonyls, the environments of these slightly inequivalent sets become more similar with increasing values of n and, at this stage, the ^{13}C n.m.r. spectrum, although poorly resolved, consists of a broad doublet due to the superposition of the terminal carbonyls resulting from different oligomers [δ(CO) 194 p.p.m., $^1J(Rh_{G/H}–CO)$ = 76 Hz] and two sets of triplets of relative intensity 2 : 1 due to the inter-triangular [δ(CO) 218 p.p.m., $^1J(Rh_{G/H}–CO)$ = 27 Hz] and intra-triangular [δ(CO) 225 p.p.m., $^1J(Rh_G–CO) = {}^1J(Rh_H–CO)$ = 50 Hz] edge-bridging carbonyls respectively; the carbide resonance appears at 285 p.p.m. but is not a well defined multiplet and there is only one rhodium resonance at −373 p.p.m. which is also broad due to the superposition of rhodium resonances from different oligomers with $n > 3$.

The next formed species, $[Ag_4\{Rh_6(CO)_{15}C\}_3]^{2-}$ (9), which is produced on further addition of $Ag[BF_4]$, has two carbide resonances of relative intensity 2 : 1 at 298.2 and 285.8 p.p.m. due to C^5 and C^6 (see Figure 3) respectively; on broad-band rhodium decoupling these resonances become a sharp doublet and triplet respectively with $^4J(C^5–C^6)$ = 7.8 Hz. This coupling which is observed when the carbide atoms are 90% ^{13}C-enriched, is rather large but arises because of the number of

* δ(C^fO) 195.3, $^1J(Rh–C^fO)$ = 79.3; δ(C^gO) 195.8, $^1J(Rh–C^gO)$ = 76.3; δ(C^hO) 223.9, $^1J(Rh–C^hO)$ = 27.5; δ(C^iO) 231.1, $^1J(Rh–C^iO)$ = 50.3; δ(C^iO) 220.4, $^1J(Rh–C^iO)$ = 30.5; δ(C^1) 272.7, $^1J(Rh_B–C^1)$ = 12.7, $^1J(Rh_C–C^1)$ = 10.7 Hz (see Figures 3 and 4, and text).

Table 3. Final atomic co-ordinates ($\times 10^4$) with estimated standard deviations in parentheses

Atom	*X/a*	*Y/b*	*Z/c*
Ag(1)	0	5 000	5 000
Rh(1)	1 544(1)	5 466(1)	5 699(1)
Rh(2)	1 165(1)	4 319(1)	4 595(1)
Rh(3)	1 115(1)	5 829(1)	4 074(1)
Rh(4)	2 542(1)	6 016(1)	3 819(1)
Rh(5)	2 972(1)	5 643(1)	5 466(1)
Rh(6)	2 603(1)	4 504(1)	4 371(1)
Ag(2)	5 000	0	0
Rh(7)	3 858(1)	10 330(1)	10 722(1)
Rh(8)	3 871(1)	10 906(1)	9 127(1)
Rh(9)	3 433(1)	9 368(1)	9 433(1)
Rh(10)	2 019(1)	9 609(1)	9 330(1)
Rh(11)	2 437(1)	10 572(1)	10 605(1)
Rh(12)	2 456(1)	11 166(1)	9 011(1)
C(O1)	1 989(6)	5 289(6)	4 672(7)
C(O2)	3 011(6)	10 333(6)	9 702(7)
C(1)	1 095(7)	5 698(8)	6 517(9)
O(1)	862(6)	5 940(6)	7 031(7)
C(2)	410(7)	3 498(8)	4 540(8)
O(2)	3(6)	2 932(7)	4 463(7)
C(3)	326(7)	6 298(8)	3 620(8)
O(3)	−90(6)	6 665(6)	3 338(6)
C(4)	3 129(7)	6 580(7)	3 143(8)
O(4)	3 483(6)	6 980(6)	2 733(6)
C(5)	3 917(7)	5 928(7)	5 975(7)
O(5)	4 507(7)	6 107(8)	6 268(8)
C(6)	3 272(7)	3 963(8)	4 153(8)
O(6)	3 687(6)	3 612(6)	4 010(6)
C(7)	1 468(7)	4 248(8)	5 872(8)
O(7)	1 558(5)	3 783(6)	6 381(6)
C(8)	836(6)	4 839(7)	3 439(8)
O(8)	609(5)	4 653(6)	2 771(6)
C(9)	1 403(7)	6 510(7)	5 072(8)
O(9)	1 464(5)	7 163(6)	5 212(6)
C(10)	3 020(7)	6 704(8)	4 785(8)
O(10)	3 286(6)	7 334(6)	4 880(6)
C(11)	3 067(7)	4 479(8)	5 580(8)
O(11)	3 325(5)	4 046(6)	6 068(7)
C(12)	2 510(7)	5 018(7)	3 206(8)
O(12)	2 560(5)	4 866(5)	2 561(6)
C(13)	2 529(7)	5 755(8)	6 439(8)
O(13)	2 713(5)	5 888(6)	7 119(6)
C(14)	1 798(7)	3 622(8)	4 287(8)
O(14)	1 708(6)	2 978(7)	4 127(7)
C(15)	1 710(6)	6 528(7)	3 306(7)
O(15)	1 581(5)	7 002(6)	2 813(6)
C(16)	4 587(7)	10 288(8)	11 584(8)
O(16)	5 001(6)	10 264(6)	12 194(7)
C(17)	4 652(7)	11 345(8)	8 637(8)
O(17)	5 068(6)	11 612(6)	8 224(7)
C(18)	3 863(7)	8 622(7)	9 080(8)
O(18)	4 054(5)	8 164(6)	8 770(6)
C(19)	1 090(8)	9 166(8)	9 010(9)
O(19)	494(8)	8 898(8)	8 771(9)
C(20)	1 811(7)	732(8)	11 254(8)
O(20)	1 433(6)	847(7)	11 693(7)
C(21)	1 863(8)	11 805(8)	8 437(9)
O(21)	1 509(7)	12 222(7)	8 053(8)
C(22)	4 223(7)	11 432(8)	10 205(8)
O(22)	4 491(5)	12 047(6)	10 447(6)
C(23)	3 529(6)	10 010(7)	8 343(8)
O(23)	3 446(5)	9 910(5)	7 645(6)
C(24)	3 552(7)	9 162(7)	10 679(8)
O(24)	3 463(5)	8 602(5)	11 151(6)
C(25)	1 960(6)	9 439(7)	10 562(8)
O(25)	1 725(5)	8 951(6)	11 013(6)
C(26)	2 492(7)	11 686(7)	10 084(8)
O(26)	2 436(5)	12 288(5)	10 320(6)
C(27)	1 953(7)	10 302(7)	8 256(8)
O(27)	1 694(5)	10 241(6)	7 572(6)
C(28)	3 293(6)	703(7)	11 477(7)
O(28)	3 430(5)	912(5)	12 172(5)
C(29)	3 290(6)	11 678(7)	8 491(8)
O(29)	3 418(5)	12 204(6)	8 034(6)
C(30)	2 462(8)	8 684(8)	9 208(9)
O(30)	2 243(6)	8 034(6)	9 098(7)
P(1)	5 179(2)	4 445(2)	8 289(2)
CA(1)	4 336(4)	4 152(5)	8 600(5)
CA(2)	4 263(4)	3 798(5)	9 363(5)
CA(3)	3 586(4)	3 547(5)	9 559(5)
CA(4)	2 983(4)	3 650(5)	8 993(5)
CA(5)	3 056(4)	4 004(5)	8 231(5)
CA(6)	3 733(4)	4 255(5)	8 034(5)
CA(7)	5 416(5)	5 463(4)	8 241(6)
CA(8)	4 919(5)	5 936(4)	8 272(6)
CA(9)	5 115(5)	6 730(4)	8 202(6)
CA(10)	5 808(5)	7 050(4)	8 101(6)
CA(11)	6 304(5)	6 577(4)	8 069(6)
CA(12)	6 108(5)	5 784(4)	8 139(6)
CA(13)	4 877(5)	5 924(5)	2 676(4)
CA(14)	4 595(5)	5 470(5)	3 300(4)
CA(15)	4 653(5)	5 766(5)	4 059(4)
CA(16)	4 994(5)	6 515(5)	4 193(4)
CA(17)	5 276(5)	6 968(5)	3 569(4)
CA(18)	5 217(5)	6 672(5)	2 810(4)
CA(19)	5 827(4)	4 077(4)	9 048(4)
CA(20)	6 120(4)	4 508(4)	9 722(4)
CA(21)	6 553(4)	4 199(4)	10 378(4)
CA(22)	6 693(4)	3 458(4)	10 361(4)
CA(23)	6 400(4)	3 027(4)	9 688(4)
CA(24)	5 967(4)	3 336(4)	9 032(4)
P(2)	126(2)	3 088(2)	−378(2)
CB(1)	302(6)	2 997(6)	703(5)
CB(2)	978(6)	2 894(6)	1 104(5)
CB(3)	1 110(6)	2 791(6)	1 949(5)
CB(4)	566(6)	2 791(6)	2 394(5)
CB(5)	−110(6)	2 895(6)	1 993(5)
CB(6)	−242(6)	2 997(6)	1 148(5)
CB(7)	93(5)	2 191(4)	−799(5)
CB(8)	397(5)	1 602(4)	−342(5)
CB(9)	355(5)	903(4)	−682(5)
CB(10)	9(5)	792(4)	−1 478(5)
CB(11)	−294(5)	1 380(4)	−1 936(5)
CB(12)	−252(5)	2 080(4)	−1 590(5)
CB(13)	−711(3)	3 376(5)	−728(5)
CB(14)	−762(3)	4 111(5)	−1 072(5)
CB(15)	−1 429(3)	4 323(5)	−1 337(5)
CB(16)	−2 045(3)	3 801(5)	−1 260(5)
CB(17)	−1 994(3)	3 066(5)	−916(5)
CB(18)	−1 327(3)	2 853(5)	−651(5)
CB(19)	795(5)	3 808(4)	−723(5)
CB(20)	1 072(5)	4 444(4)	−263(5)
CB(21)	1 494(5)	5 072(4)	−589(5)
CB(22)	1 639(5)	5 064(4)	−1 374(5)
CB(23)	1 363(5)	4 428(4)	−1 833(5)
CB(24)	941(5)	3 800(4)	−1 508(5)
P(3)	2 084(2)	9 542(3)	4 864(3)
CC(1)	2 189(5)	8 928(5)	5 746(5)
CC(2)	2 741(5)	8 499(5)	5 902(5)
CC(3)	2 817(5)	8 016(5)	6 602(5)
CC(4)	2 340(5)	7 961(5)	7 146(5)
CC(5)	1 788(5)	8 390(5)	6 990(5)
CC(6)	1 712(5)	8 873(5)	6 290(5)
CC(7)	2 417(6)	10 516(6)	5 090(8)
CC(8)	2 582(6)	11 058(6)	4 471(8)
CC(9)	2 803(6)	11 826(6)	4 641(8)
CC(10)	2 858(6)	12 052(6)	5 430(8)
CC(11)	2 692(6)	11 510(6)	6 049(8)
CC(12)	2 472(6)	10 742(6)	5 879(8)
CC(13)	2 589(6)	9 303(6)	4 150(6)
CC(14)	2 253(6)	8 858(6)	3 500(6)
CC(15)	2 652(6)	8 655(6)	2 962(6)

Table 3 (*continued*)

Atom	X/a	Y/b	Z/c	Atom	X/a	Y/b	Z/c
CC(16)	3 387(6)	8 897(6)	3 073(6)	CC(21)	13(5)	8 642(7)	4 148(7)
CC(17)	3 723(6)	9 342(6)	3 723(6)	CC(22)	−279(5)	9 269(7)	3 765(7)
CC(18)	3 324(6)	9 545(6)	4 262(6)	CC(23)	148(5)	9 986(7)	3 725(7)
CC(19)	1 160(5)	9 449(7)	4 450(7)	CC(24)	868(5)	10 076(7)	4 067(7)
CC(20)	733(5)	8 732(7)	4 490(7)				

different pathways available for transmission of spin–spin coupling and provides strong evidence for the formation of such oligomers. Similar large long-range coupling constants arising from multiple-path mechanisms have recently been found in bicyclic hydrocarbons.[8] At this stage, the rhodium n.m.r. spectrum at −80 °C consists of three equally intense resonances at −383, −377, and −371 p.p.m.; this is consistent with the structure of (9) but assignments are not possible. Further addition of $Ag[BF_4]$ to the acetone solution of (9) at −80 °C results in the formation of $[Ag_3\{Rh_6(CO)_{15}C\}_2]^-$ (10) and $[Ag_2\{Rh_6(CO)_{15}C\}]$ (11). Direct rhodium n.m.r. spectra on (10) show two equally intense resonances (−378 and −381 p.p.m.) and the carbide resonance (C^7) appears at 300.8 p.p.m. Formation of (11) is complete on addition of excess $Ag[BF_4]$ $\{Ag^+ : [Rh_6(CO)_{15}C]^{2-} = 3 : 1\}$ and spectra free from other oligomers are obtained. Thus the ^{13}C n.m.r. spectrum in the carbonyl region consists of a doublet due to the terminal carbonyls [δ(CO) 193.5 p.p.m., $^1J(Rh–CO)$ = 76.3 Hz] and two triplets of intensity 2 : 1 due to the inter-triangular [δ(CO) 219.4 p.p.m., $^1J(Rh–CO)$ = 27.5 Hz] and intra-triangular [δ(CO) 227.9 p.p.m., $^1J(Rh–CO)$ = 51.9 Hz] edge-bridging carbonyls respectively; the carbide resonance, due to C^8, appears at 300.3 p.p.m. as a sharp septet $^1J(Rh–C^8)$ = 12.7 Hz and a single rhodium resonance is observed at $\delta(Rh_N)$ = −384.9 p.p.m.

Consideration of the n.m.r. data shows that there is a shift of $\delta(CO)_{mean}$ on going from (5) (215.4 p.p.m.) to (11) (210.7 p.p.m.) due to the reduced charge on the cluster, while the carbide resonance shifts progressively to lower field on going from (5) to (11). The rather small change in $\delta(C_{carbide})$ found for $[Rh_6(CO)_{15}C]^{2-}$ on adduct formation is similar to the situation now found [9] on addition of electrophiles to $[Ru_6(CO)_{16}C]^{2-}$.* Little change in the values of $J(Rh–CO)$ is found on going from (5) to (11), which is consistent with the minor variation in $d(Rh–CO)$ found for (5) and (6). Capping one triangular face of (5) with Ag^+ produces a significant shift in δ(Rh) whereas δ(Rh) for the uncapped face remains close to $\delta(Rh_A)$ in (5) [*e.g.* $\delta(Rh_A)$ in (5) at −313 p.p.m. shifts to −278 (Rh_B) and −423 p.p.m. (Rh_C) in (6)]. When both faces of the same trigonal prism are capped by Ag^+ then δ(Rh) is within the range −373 [for (8)] to −394 p.p.m. [for (11)] and it therefore seems reasonable to assign the rhodium resonances for (7) found at −279, −363, and −433 p.p.m. to the uncapped face, Rh_D, to the central Rh_6 trigonal prism, Rh_F, and to the Rh_E face of the monocapped trigonal prism respectively (see above).

It is of course impossible to deduce from n.m.r. measurements whether or not the trigonal prismatic units in (7)–(10) are staggered or eclipsed with respect to each other but it seems probable, because of steric constraints, that they are staggered as found for (6) by *X*-ray crystallography.

The silver-capped clusters (6) to (11) are relatively stable in solution at room temperature in the absence of oxygen but, in the presence of excess Ag^+, undergo further reaction, which is presently under investigation.

* The exceptional carbide shift on going from $[Ru_6(CO)_{16}]^{2-}$ (288 p.p.m.) [10] to $[\{Cu(NCMe)\}_2\{Rh_6(CO)_{16}C\}]$ (459 p.p.m.) [11] has now been shown to be incorrect since remeasurement of the carbide chemical shift in $[Ru_6(CO)_{16}C]^{2-}$ gives a value of 458.9 p.p.m.[9]

Experimental

^{13}C, ^{13}C-{^{103}Rh}, ^{31}P, and ^{103}Rh measurements were made as described previously.[2,12–14] Carbon-13, ^{31}P, and ^{103}Rh chemical shifts are referenced to $SiMe_4$, external H_3PO_4 (80% in D_2O), and 3.16 MHz (equals 0 p.p.m. at such a magnetic field that the protons in $SiMe_4$ in $CDCl_3$ solution resonate at exactly 100 MHz) respectively; high-frequency shifts are positive.

I.r. spectra were recorded using 0.1-mm CaF_2 cells on a Perkin-Elmer 683 spectrometer equipped with a data handling station. Atomic absorption measurements, in order to determine the concentration of rhodium and silver in solution, were made on a Pye-Unicam SP 90 spectrometer.

Carbon-13 (^{13}CO) enrichments (*ca.* 30—40%) were carried out using standard vacuum-line techniques and all operations were carried out under a nitrogen atmosphere.

Published methods were used to prepare $[Au(PEt_3)Cl]$,[15] $[\{Ag(PEt_3)Br\}_4]$,[16] and $K_2[Rh_6(CO)_{15}C]$.[17]

Carbon-13 (^{13}CO) *Enrichment* (ca. 30—40%) *of* $[Rh_6(CO)_{15}C]^{2-}$.—A solution of $K_2[Rh_6(CO)_{15}C]$ in tetrahydrofuran was boiled under an atmosphere of ^{13}CO for 2 h and then allowed to cool, with stirring, under the same atmosphere for *ca.* 12 h. Removal of the CO and solvent followed by dissolution of the residue in methanol and addition of a methanol solution of benzyltrimethylammonium chloride gave a precipitate, which was filtered off, dried and recrystallised from acetone–propan-2-ol to give yellow crystals of $[NMe_3(CH_2Ph)]_2[Rh_6(^{13}CO)_{15}C]$.

$[NMe_3(CH_2Ph)]_2[Rh_6(CO)_{15}{}^{13}C]$.—A solution of $[Rh_4(CO)_{12}]$ (0.5 g) in diglyme (30 cm^3) was stirred with potassium metal (*ca.* 1 g) under an atmosphere of CO for two days. The solution was filtered and the rhodium content of the filtrate, as $K[Rh(CO)_4]$, was obtained by atomic absorption. To this solution was added exactly ⅛ mol of CCl_4 (90% ^{13}C) using a microsyringe and the resultant product, $K_2[Rh_6(CO)_{15}{}^{13}C]$, was precipitated with hexane and recrystallised from acetone–diglyme. Conversion of the potassium salt to $[NMe_3(CH_2Ph)]_2[Rh_6(CO)_{15}{}^{13}C]$ was carried out as described above.

$[NMe_3(CH_2Ph)][\{M(PEt_3)\}\{Rh_6(CO)_{15}C\}]$ (M = Ag *or* Au).—To a solution of $[NMe_3(CH_2Ph)]_2[Rh_6(CO)_{15}C]$ (0.1 mmol) in acetone was added at room temperature a solution of either $[\{Ag(PEt_3)Br\}_4]$ (0.05 mmol) or $[Au(PEt_3)Cl]$ (0.2 mmol). After filtering off the precipitated $[NMe_3(CH_2Ph)]X$ (X = Cl or Br), the solution was used directly for multinuclear n.m.r. studies. It should be noted that the silver adduct is unstable in solution at room temperature but is stable for prolonged periods at −70 °C. The ν(CO) region of the i.r. spectra of both the silver and gold adducts in acetone solution were identical (2 006s and 1 868s cm^{-1}).

$[NMe_3(CH_2Ph)][\{Cu(NCMe)\}\{Rh_6(CO)_{15}C\}]$ *and* $[\{Cu(NCMe)\}_2\{Rh_6(CO)_{15}C\}]$.—These compounds were prepared

by the addition of an acetone solution of $[Cu(NCMe)][BF_4]$ to an acetone solution of $[NMe_3(CH_2Ph)]_2[Rh_6(CO)_{15}C]$. For $[NMe_3(CH_2Ph)][\{Cu(NCMe)\}\{Rh_6(CO)_{15}C\}]$ in acetone, $\nu(CO) = 2\,010$s and 1 863s cm^{-1} and for $[\{Cu(NCMe)\}_2\{Rh_6(CO)_{15}C\}]$ in acetone, $\nu(CO) = 2\,027$s and 1 881s cm^{-1}. N.m.r. data for $[NMe_3(CH_2Ph)][\{Cu(NCMe)\}\{Rh_6(CO)_{15}C\}]$ in acetone: ^{13}C at −83 °C, δ 194.3 (d, $J = 79.3$, 6 CO_t), 221.4 (t, $J = 29.0$, 6 μ-CO), 230.5 (t, $J = 51.9$, 3 μ-CO), and 281.8 p.p.m. (septet, $J = 13.2$ Hz, carbide); ^{103}Rh at −83 °C, δ −307 (s) p.p.m. N.m.r. data for $[\{Cu(NCMe)\}_2\{Rh_6(CO)_{15}C\}]$ in acetone: ^{13}C at 25 °C, δ 193.4 (d, J 76.3, 6 CO_t), 217.6 (t, $J = 27.5$, 6 μ-CO), 225.0 (d, $J = 50.3$, 3 μ-CO), and 300.3 p.p.m. (septet, $J = 12.7$ Hz, carbide); ^{103}Rh at 25 °C and −70 °C, δ −441 (s) and −450 (s) p.p.m. respectively.

Reaction of $Ag[BF_4]$ *with* $[NMe_3(CH_2Ph)]_2[Rh_6(CO)_{15}C]$.—To an acetone solution of $[NMe_3(CH_2Ph)]_2[Rh_6(CO)_{15}C]$ was added with a microsyringe a standard solution of $Ag[BF_4]$ in acetone to give solutions containing the molar ratios shown in Figure 3. Each incremental addition produced an immediate reaction and the solutions were used directly for n.m.r. measurements.

$[PPh_4]_3[Ag\{Rh_6(CO)_{15}C\}_2]$.—An acetone solution of $Ag[BF_4]$ (0.0155 mol dm^{-3}) was added to a solution of $[PPh_4]_2[Rh_6(CO)_{15}C]$ (0.150 g, 0.087 mmol) in acetone (8 cm^3) under nitrogen until the bands due to $[PPh_4]_2[Rh_6(CO)_{15}C]$ had disappeared and the spectrum showed only bands at 2 005vs, 1 861s, 1 830m, and 1 815m cm^{-1} (*ca.* 3 cm^3 of solution was required). The product was precipitated by adding hexane (30 cm^3), filtered off, washed with hexane (3 × 5 cm^3) and dried *in vacuo*. The yield based on Rh was *ca.* 75%.

Crystals of the product suitable for *X*-ray analysis were obtained by recrystallization, using the slow diffusion technique, from a solution of the crude product in acetone–methyl formate (3.0 : 0.1 cm^3) by careful addition of propan-2-ol (12 cm^3) (Found: C, 38.9; H, 2.0. Calc. for $C_{104}H_{60}AgO_{30}P_3Rh_{12}$: C, 38.7; H, 1.9%).

Crystal data. $C_{104}H_{60}AgO_{30}P_3Rh_{12}$, $M = 3\,225.3$, Triclinic, $a = 19.359(2)$, $b = 17.786(2)$, $c = 16.753(2)$ Å, $\alpha = 85.105(2)$, $\beta = 100.337(2)$, $\gamma = 100.194(2)°$, $U = 5\,576.6$ Å^3, $D_m = 1.95$, $Z = 2$, $D_c = 1.92$ g cm^{-3}, space group $P\bar{1}$ (no. 2), $F(000) = 3\,112$, Mo-K_α radiation, $\lambda = 0.710\,69$ Å, μ(Mo-K_α) = 18.3 cm^{-1}.

Intensity measurements. A suitable crystal of dimensions 0.20 × 0.25 × 0.18 mm was mounted on a Philips PW1100 diffractometer. Diffraction intensities were measured in four octants of the reciprocal lattice in the range $2 < \theta < 22°$, by the ω-scan method, with scan interval 1.2°, and speed 0.04° s^{-1}. The background was measured on both sides of the reflections for a total time equal to the peak scanning time. 13 685 Reflections were collected, 10 218 of which $[F_o > 5\sigma(F_o)]$ were used for the structure solution and refinement. The integrated intensities were reduced to F_o values, and an experimental correction for absorption was applied.

The SHELX [18] package of crystallographic programs was used for the computations. The structure was solved by direct methods, whose application revealed two independent prisms of rhodium atoms and two silver atoms placed on inversion centres. These findings were rationalized as two centrosymmetric and semi-independent $AgRh_{12}$ clusters with the silver atoms bridging two prismatic units through the triangular faces. A difference-Fourier map computed after a refinement of the metal atoms showed all the light atoms. The structure was refined by least-squares calculations. The metal atoms were allowed to vibrate anisotropically, all the light atoms, including the phosphorus atoms in the cations, were refined isotropically. The phenyl rings were treated as rigid groups (C–C 1.395 Å, C–C–C 120°), the hydrogen atoms were omitted. The final agreement indices were $R = 0.063$ and $R' = 0.070$. A final difference-Fourier map showed residual peaks lower than 1.0 e Å^{-3} in the vicinity of the heavy atoms. The co-ordinates of all the refined atoms are reported in Table 3, bond distances and relevant angles in Table 2.

Acknowledgements

We thank S.E.R.C. and C.N.R. for financial support, and S.E.R.C. for a research fellowship (to L. S.) and for high-field n.m.r. facilities. We also thank Dr. I. H. Sadler for carrying out the direct ^{103}Rh n.m.r. measurements.

References

1 P. Chini, *J. Organomet. Chem.*, 1980, **200**, 37.
2 B. T. Heaton, L. Strona, S. Martinengo, D. Strumolo, R. J. Goodfellow, and I. H. Sadler, *J. Chem. Soc., Dalton Trans.*, 1982, 1499.
3 V. G. Albano, D. Braga, S. Martinengo, P. Chini, M. Sansoni, and D. Strumolo, *J. Chem. Soc., Dalton Trans.*, 1980, 52.
4 V. G. Albano, P. Chini, S. Martinengo, D. J. A. McCaffrey, D. Strumolo, and B. T. Heaton, *J. Am. Chem. Soc.*, 1974, **96**, 8106.
5 V. G. Albano, M. Sansoni, P. Chini, and S. Martinengo, *J. Chem. Soc., Dalton Trans.*, 1973, 651.
6 A. F. Wells, 'Structural Inorganic Chemistry,' Clarendon Press, Oxford, 1975.
7 J. A. Creighton, R. Della Pergola, B. T. Heaton, S. Martinengo, L. Strona, and D. A. Willis, *J. Chem. Soc., Chem. Commun.*, 1982, 864.
8 M. Klessinger and J.-H. Cho, *Angew. Chem., Int. Ed. Engl.*, 1982, **21**, 764 and refs. therein.
9 J. S. Bradley, personal communication.
10 J. S. Bradley, G. B. Ansell, and E. W. Hill, *J. Organomet. Chem.*, 1980, **184**, C33.
11 J. S. Bradley, R. L. Pruett, E. Hill, G. B. Ansell, M. E. Leonowicz, and M. A. Modrick, *Organometallics*, 1982, **1**, 748.
12 G. Longoni, B. T. Heaton, and P. Chini, *J. Chem. Soc., Dalton Trans.*, 1980, 1537.
13 C. Brown, B. T. Heaton, L. Longhetti, W. T. Povey, and D. O. Smith, *J. Organomet. Chem.*, 1980, **192**, 93.
14 B. T. Heaton, L. Longhetti, D. M. P. Mingos, C. E. Briant, P. C. Minshall, B. C. Theobald, L. Garlaschelli, and U. Sartorelli, *J. Organomet. Chem.*, 1981, **213**, 333.
15 F. G. Mann, A. F. Wells, and D. Purdia, *J. Chem. Soc.*, 1937, **386**, 1828.
16 B. K. Teo and J. C. Calabrese, *J. Am. Chem. Soc.*, 1975, **97**, 1256.
17 S. Martinengo, D. Strumolo, and P. Chini, *Inorg. Synth.*, 1980, **20**, 212.
18 G. Sheldrick, SHELX 75 System of Computer Programs, Cambridge, 1975.

Received 29*th December* 1982; *Paper* 2/2172